Journal of The Electrochemical Society, **157** (3) H304-H307 (2010)
0013-4651/2010/157(3)/H304/4/$28.00 © The Electrochemical Society

Effects of Lens Shape on GaN Grown on Microlens Patterned Sapphire Substrates by Metallorganic Chemical Vapor Deposition

Hung-Cheng Lin,[a] Hsueh-Hsing Liu,[a] Geng-Yen Lee,[a] Jen-Inn Chyi,[a,b,c,*,z] Chang-Ming Lu,[d] Chih-Wei Chao,[d] Te-Chung Wang,[d] Chun-Jong Chang,[d] and Solomon W. S. Chi[d]

[a]*Department of Electrical Engineering and* [b]*Department of Optics and Photonics, National Central University, Jhongli 32001, Taiwan*
[c]*Research Center for Applied Sciences, Academia Sinica, Taipei 11529, Taiwan*
[d]*Lextar Electronics Corporation, Hsinchu 30075, Taiwan*

The epitaxial growth of GaN on patterned *c*-plane sapphire substrates having microlenses with a flat top, a dull tip, or a sharp tip is carried out. The growth mode, dislocation density, residual strain, and optical properties of GaN are investigated and correlated with the shape of the microlens. Because the growth of GaN does not take place on top of the microlens with a sharp tip, this type of patterned substrate leads to a wider low dislocation density lateral growth region, while it also gives rise to a higher compressive residual strain in GaN. For GaN grown on the microlens with a dull tip, many dislocations appear, resulting from the extra facets on the lens. It, however, has the lowest compressive strain among the samples studied. This work provides a guideline for preparing microlens patterned sapphire substrates for potential applications in high brightness InGaN light emitting diodes as both dislocation density and strain influence their internal quantum efficiency.
 [DOI: 10.1149/1.3280949]

Manuscript submitted August 17, 2009; revised manuscript received December 7, 2009. Published January 12, 2010.

High power and high efficiency InGaN light emitting diodes (LEDs) have been intensively pursued recently for energy saving lighting as well as for other versatile applications. However, the external quantum efficiency of InGaN LEDs still falls short of what is expected. Improving both internal quantum efficiency and light extraction efficiency has thus become the focus of research. The former involves material quality improvement and epilayer structure design, while the latter concerns the escape of photons out of the semiconductor chip and packaging materials. Due to the large lattice mismatch (~16%) between GaN and sapphire, the resultant high threading dislocation density (typically in the range of 10^9–10^{10} cm^{-2}) of nitride LEDs grown on sapphire substrates severely limits their internal quantum efficiency. There have been several techniques, such as epitaxial lateral overgrowth,[1-3] SiN nanonetwork,[4] and porous TiN,[5] proposed to reduce the dislocations. Although these techniques can effectively improve crystalline quality, the two-step regrowth procedures involved make these approaches rather time-consuming and tend to introduce contamination in the epilayers. However, patterned sapphire substrates (PSSs) fabricated by dry or wet etching have attracted much attention for a high production yield because the growth on these substrates proceeds in a single growth process without any dielectric mask layer or interruption. The use of PSSs reduces the threading dislocation density in GaN epilayers as well as enhances the light extraction efficiency of LEDs. To date, several types of PSSs with one-dimensional stripe,[6] two-dimensional bump,[7] hole,[8] pyramid,[9] and lens[10-12] patterns have been developed. The pattern depth and shape also affect the epitaxial growth mode, which determines the structural and optical properties of the LEDs grown on stripe PSSs.[13,14] However, the growth mechanism and property of GaN on microlens PSSs are not well understood as previous studies primarily focused on the comparison of LEDs grown on flat and PSSs.[10-12] In this work, we prepare PSSs with microlenses of different shapes. The effects of the lens shape on the growth mode and dislocation density of the overgrown GaN are systematically investigated. Because strain engineering is a key process in fabricating InGaN quantum well LEDs, particularly green LEDs, which have a high indium content and thus a high piezoelectric field in the well, we have also looked into the residual strain in GaN grown on these PPSs and correlated it with its growth mode and dislocation density.

* Electrochemical Society Active Member.
z E-mail: chyi@ee.ncu.edu.tw

Experimental

The PSSs were prepared by inductively coupled plasma etching. The surface morphology of the PSS surface was characterized by atomic force microscopy, as shown in Fig. 1. Three types of microlenses were prepared with their diameter/spacing/depth being 3/1.5/1.5, 3/1.5/1.6, and 3/2/1.7 μm and were designated to be types I, II, and III, respectively. On the type-I PSS, the microlens had a small flat (0001) *c*-plane surface on the top, and its sidewall had a slanted angle of 65° with respect to the (0001) *c*-plane. On the type-II PSS, the microlens had a dull tip, and its sidewalls had slanted angles of 23 and 65° with respect to the (0001) *c*-plane. On the type-III PSS, the microlens was like a pyramid with a sharp tip. Its sidewalls had a slanted angle of 57° with respect to the (0001) *c*-plane.

The epitaxial growth was carried out in a low pressure metallorganic chemical vapor deposition horizontal reactor. The growth was performed using a two-step process, which started with a relatively high V/III ratio (2500) and a high pressure (250 mbar) to promote the vertical growth in the first hour, and then proceeded to a higher substrate temperature (from 1100 to 1140°C) and to a lower pressure (200 mbar) to enhance the lateral growth. The optical and structural properties of the GaN films were assessed by cathodoluminescence (CL), scanning electron microscopy (SEM), transmission electron microscopy (TEM), X-ray diffraction (XRD), photoluminescence (PL) measurement, and micro-Raman (μ-Raman) scattering.

Results and Discussion

Growth mode analysis.— Shown in Fig. 2a-c is the growth evolution of GaN on the microlens PSSs revealed by SEM images for growth times of 20, 60, and 180 min, respectively. The growth selectively proceeds with GaN islands nucleating at specific locations rendered by the pattern. In the initial growth stage of the GaN on type-I microlens PSS, i.e., the vertical growth enhanced stage, GaN grows on both the top of the microlens and the floor area, as shown in Fig. 2 (1a). The angle of the side facets for GaN on the microlens and floor area is about 62 and 58°, indicating that they are the $\{1\bar{1}01\}$ and $\{11\bar{2}2\}$ facets, respectively. Because the lateral growth rate of the $\{1\bar{1}01\}$ facet of GaN is not sensitive to the reactor pressure and the growth temperature as that of the $\{11\bar{2}2\}$ facet,[15] the

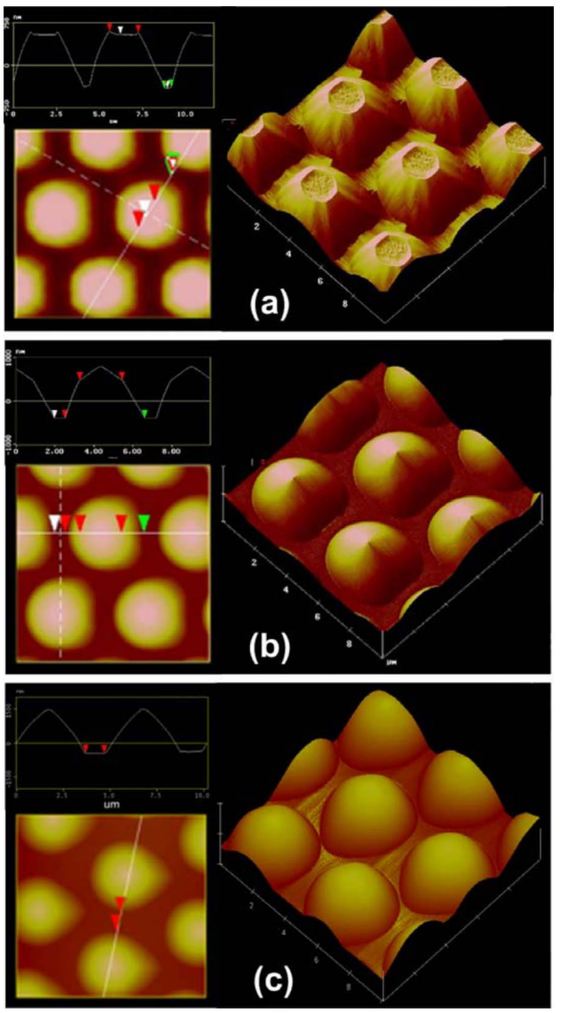

Figure 1. (Color online) Atomic force microscopic images (10×10 μm) of the surface morphology of (a) type-I, (b) type-II, and (c) type-III microlens. Their diameter/spacing/depth are about 3/1.5/1.5, 3/1.5/1.6, and 3/2/1.7 μm.

$\{11\bar{2}2\}$ facets move faster laterally than the $\{1\bar{1}01\}$ facets of the hexagonal GaN pyramid on the microlens as growth proceeds in the lateral growth enhanced stage. Six v-shaped defectlike trenches around the hexagonal pyramid are thus formed, as shown in Fig. 2 (1b). A GaN epilayer with a smooth surface is eventually achieved with time, as shown in Fig. 2 (1c). As for the type-II microlens PSS, GaN grows in the same mode as in type-I PSS, as revealed by Fig. 2 [(2a)-(2c)]. Due to the lack of a large *c*-plane area on top of the microlens and different growth modes for various facets, less symmetric GaN pyramids are formed and lead to nonuniform trenches around the sidewall of the pyramids. In spite of this imperfection, GaN with a smooth surface can still be obtained on the type-II PSS. For the type-III PSS, GaN does not grow on top of the microlens at all, as depicted in Fig. 2 [(3a)-(3b)]. This is attributed to the lack of *c*-plane facets for GaN to nucleate and grow. A flat featureless GaN film is achieved after the coalescence of the lateral growth region over the microlens, as shown in Fig. 2 (3c).

Shown in Fig. 3a-c are the cross-sectional SEM images of GaN grown on the three PSSs before coalescence. Based on the observations above, the growth mode and the evolution of GaN on type-I, -II, and -III PSSs are plotted in Fig. 3d-f, respectively. These results confirm our postulation that the microlens with a sharp tip prohibits the nucleation and growth of GaN on its top and leads to a wider

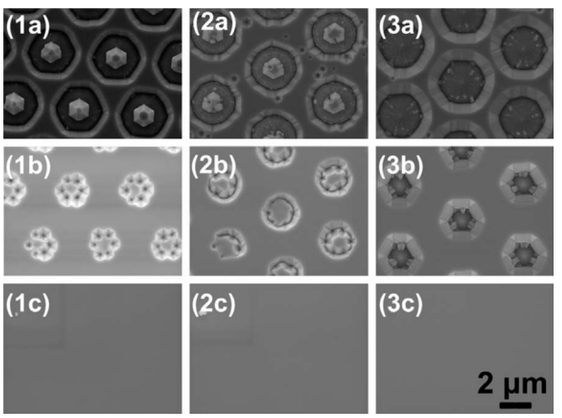

Figure 2. SEM images of GaN epilayers grown on type [(1a)-(1c)] I, [(2a)-(2c)] II, and [(3a)-(3c)] III microlens PSSs for growth times of 20, 60, and 180 min.

lateral growth region. It is also expected to result in a lower overall threading dislocation density in GaN as the lateral growth region is often of low dislocation density.[16]

Material characterization of GaN grown on microlens PSS.— The improvement on crystalline quality by using the microlens PSSs is verified by XRD, PL, etch pit density (EPD), and CL measurements on 5 μm thick GaN samples. The results of these measurements are summarized in Table I. As expected, XRD shows that the full width at half-maximum (fwhm) of the rocking curve for GaN grown on type-III PSS decreases in both the symmetric (002) and asymmetric (102) reflections compared to those grown on the type-I and -II ones. The fwhm's of the symmetric (002) reflections of the type-I and -II samples are comparable, but the fwhm of the asymmetric (102) reflection of the type-II sample is larger than that of the type-I sample. It has been reported that for GaN films on (0001) *c*-plane sapphire, the fwhm of the symmetric rocking curve is broadened by screw and mixed dislocations, while the asymmetric one is broadened by the edge component of threading dislocations.[17] The measured X-ray rocking curves indicate that a relatively higher edge dislocation density is expected for GaN on type-II PSS. The lower dislocation density for the GaN layer grown on type-III PSS is also confirmed by other means. Its EPD is reduced from 1.7×10^8 to 0.9×10^8 cm^{-2} compared to GaN grown on type-I PSS.

For more insight into the structural properties of GaN, CL and TEM are employed to observe the dislocation distribution in these samples. Figure 4 shows the plan-view CL intensity spatial mapping and the cross-sectional TEM images of GaN grown on type-I, -II, and -III microlens PSSs. The dashed circles in Fig. 4a-c mark the location of the microlenses underneath. The CL mapping shows the integrated intensity of the 366 nm GaN band-edge emission. Many

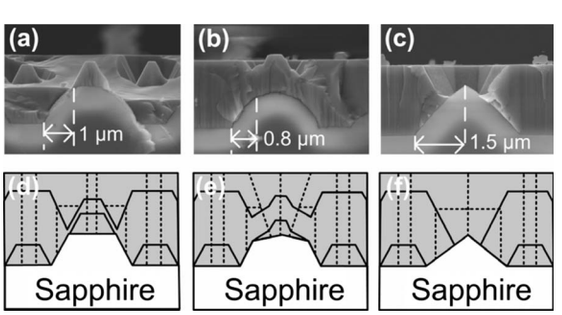

Figure 3. [(a)-(c)] Cross-sectional SEM images and [(d)-(f)] schematic growth modes of GaN grown on type-I, -II, and -III microlens PSSs.

Table I. Results of XRD, PL, EPD, and CL measurements on 5 μm thick GaN epilayers grown on type-I, -II, and -III microlens PSSs.

Sample	XRD fwhm (arcsec) (002)	XRD fwhm (arcsec) (102)	PL fwhm (meV)	EPD (cm^{-2})	CL pattern density (cm^{-2})
Type I	241	209	63	1.7×10^8	1×10^8
Type II	243	223	67	2.3×10^8	2×10^8
Type III	220	183	61	9.0×10^7	8×10^7

dark areas mainly appear at the center and the surroundings of the microlenses due to nonradiative recombination at the dislocation-rich regions.[18] The bright regions, which represent the areas of low dislocation density, appear at the places corresponding to the sidewalls of the microlenses. This is consistent with the cross-sectional TEM images shown in Fig. 4d-f. In these images, three regions denoted as A, B, and C are highlighted. In region A, one can observe that many dislocations are present at the GaN/sapphire interface, where the GaN growth starts. In region B, the density of dislocation is low because threading dislocations bend during the vertical growth stage as they meet the inclined $\{11\bar{2}2\}$ facets. In region C, some new threading dislocations are generated due to the coalescence of two growth fronts. In all, a wider bright region in the CL mapping as well as a lower dislocation density in the TEM micrograph are observed on the GaN grown on type-III microlens PSS, which agrees with the results shown in Table I. The dislocation distribution around the type-II microlens is rather different from that of the other two samples when comparing Fig. 4d-f. There are many dislocations generated perpendicular to the slanted facets on the dull tip. This phenomenon is similar to what is observed on the growth of GaN on misoriented *c*-plane sapphire by metallorganic chemical vapor deposition and hydride vapor phase epitaxy.[19,20]

As strain is critical to the internal quantum efficiency of InGaN-based LEDs, the residual strain in GaN on these PSSs is also evaluated by room-temperature μ-Raman measurement. For this measurement, the 514.5 nm line of an Ar^+ laser is used as the excitation source. Figure 5 shows the E_2 high mode of a freestanding GaN substrate and the GaN grown on type-I, -II, and -III PSSs, which are located at 566.8, 568.6, 568.2, and 569.0 cm^{-1}, respectively. Assuming that the freestanding GaN is strain free, the compressive stress in the GaN films can be estimated by the linear expression $\Delta\omega = K\sigma_{xx}$ cm^{-1} GPa^{-1}, where $\Delta\omega$ is the wavenumber shift of the E_2 phonon peak with respect to that of the GaN substrate, and the K value of 2.56 is adopted in our calculation.[21] Accordingly, the compressive stress in GaN on type I, II, and III microlens PSSs is determined to be −0.73, −0.56, −0.89 GPa, respectively. The residual strain in the GaN films can be obtained using the expression $\sigma_{xx} = M_f\varepsilon_{xx}$, where M_f is the biaxial modulus of the substrate (M_f = 449.6 GPa).[22] The values are -1.623×10^{-3}, -1.246×10^{-3}, and -1.980×10^{-3} for the type-I, -II, and -III GaN samples, respectively. The data are also verified by XRD, which gives the lattice constant c of the three samples to be 5.1902, 5.1887, and 5.1906 Å, respectively. The strain component in the growth direction can be determined through the expression $\varepsilon_{zz} = (c - c_o)/c_o$, where c_o is 5.185 Å. The strain in the basal plane can then be obtained by $\varepsilon_{zz} = -D(x)\varepsilon_{xx}$, with $D(x) = 2[C_{13}(x)/C_{33}(x)]$, where the elastic constants of GaN $C_{13}(x)$ is 103 GPa and $C_{33}(x)$ is 405 GPa.[23] The strains of the three samples are calculated to be -1.968×10^{-3}, -1.414×10^{-3}, and -2.134×10^{-3}, respectively. Although there are discrepancies in the absolute value of the strain estimated by μ-Raman and XRD, the trend is consistent with the strain in GaN grown on type-II PSS being 51–59% lower than that in the GaN on type-III PSS. The lower residual compressive strain in the GaN grown on type-II microlens PSS is attributed to its higher dislocation density, which induces higher tensile growth stress due to island coalescence at growth temperature.[22,24] As the sample is cooled to room temperature, the mismatch of the thermal expansion coeffi-

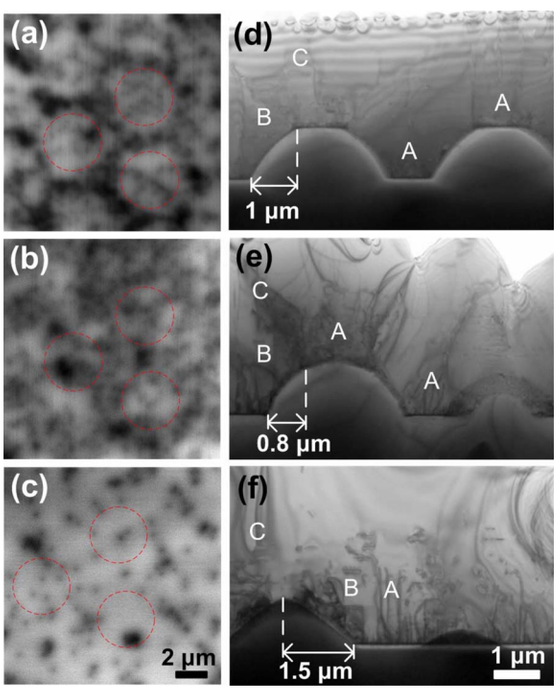

Figure 4. (Color online) [(a)-(c)] Plan view CL mapping and [(d)-(f)] cross-sectional TEM images of 5 μm thick GaN layer grown on type-I, -II, and -III microlens PSSs.

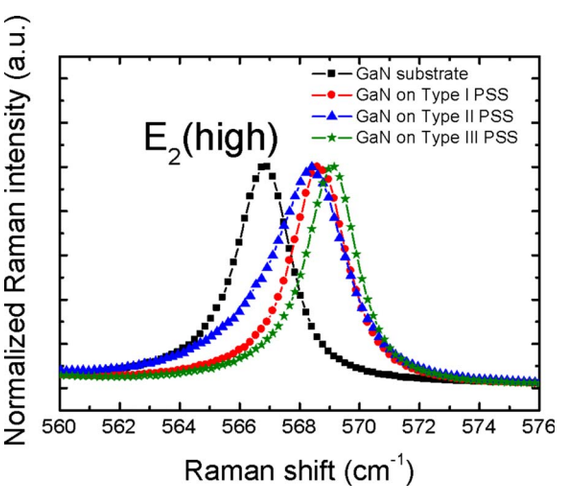

Figure 5. (Color online) E_2 high phonon peak of 250 μm thick GaN substrate and 5 μm thick GaN grown on type-I, -II, and -III microlens PSSs. Higher wavenumber means higher compressive strain.

cient between GaN and sapphire makes the GaN less compressively strained. However, the GaN grown on the type-III substrate has the lowest dislocation density; it should have the lowest tensile strain and thus exhibit the largest compressive strain at room temperature as observed.

Conclusions

In summary, we have carried out GaN growth on PSSs with three different shapes of microlenses by metallorganic vapor phase deposition. The shape of the microlens affects the growth mode and the structural and optical properties of GaN. As GaN preferentially grows on *c*-plane sapphire, no growth takes place on the microlens with a sharp tip (type-III PSSs). This leads to a wider lateral growth region of low dislocation density than the other two cases. However, GaN grown on microlens with a dull tip (type-II PSSs) has high dislocation density, especially at the slanted sidewalls on the tip, resembling the growth on misoriented sapphire. This work also reveals that GaN grown on microlens with a sharp tip exhibits the highest residual compressive strain among the three samples. It is attributed to its low tensile strain at growth temperature. Compressive strain then develops when the sample is cooled to room temperature due to the mismatch of the thermal expansion coefficient between GaN and sapphire. While for GaN grown on the microlens with a dull tip, high density of dislocations induces large tensile growth stress at a growth temperature and results in a smaller compressive residual strain after cooling to room temperature. This work provides a guideline for preparing microlens PSSs for high brightness InGaN LEDs as both dislocation density and strain influence their internal quantum efficiency.

Acknowledgments

The authors thank Dr. G.-T. Chen and Y.-C. Liu for their assistance in material characterization. The project is partly supported by the National Science Council of Taiwan under contract no. NSC 96-2628-E-072-MY3.

National Central University assisted in meeting the publication costs of this article.

References

1. R. W. McClelland, C. O. Bozler, and J. C. C. Fan, *Appl. Phys. Lett.*, **37**, 560 (1980).
2. Y. Kato, S. Kitamura, K. Hiramatsu, and N. Sawaki, *J. Cryst. Growth*, **144**, 133 (1994).
3. T. S. Zheleva, O.-H. Nam, M. D. Bremser, and R. F. Davis, *Appl. Phys. Lett.*, **71**, 2472 (1997).
4. S. Sakai, T. Wang, Y. Morishima, and Y. Naoi, *J. Cryst. Growth*, **221**, 334 (2000).
5. Y. Fu, Y. T. Moon, F. Yun, Ü. Özgür, J. Q. Xie, S. Dogan, H. Morkoç, C. K. Inoki, T. S. Kuan, L. Zhou, et al., *Appl. Phys. Lett.*, **86**, 043108 (2005).
6. K. Tadatomo, H. Okagawa, Y. Ohuchi, T. Tsunekawa, Y. Imada, M. Kato, and T. Taguchi, *Jpn. J. Appl. Phys., Part 2*, **40**, L583 (2001).
7. M. Yamada, T. Mitani, Y. Narukawa, S. Shioji, I. Niki, S. Sonobe, K. Deguchi, M. Sano, and T. Mukai, *Jpn. J. Appl. Phys., Part 2*, **41**, L1431 (2002).
8. D. S. Wuu, W. K. Wang, W. C. Shih, R. H. Horng, C. E. Lee, W. Y. Lin, and J. S. Fang, *IEEE Photon. Technol. Lett.*, **17**, 288 (2005).
9. H.-C. Lin, R.-S. Lin, J.-I. Chyi, and C.-M. Lee, *IEEE Photon. Technol. Lett.*, **20**, 1621 (2008).
10. H. W. Choi, C. Liu, E. Gu, G. McConnell, J. M. Girkin, I. M. Watson, and M. D. Dawson, *Appl. Phys. Lett.*, **84**, 2253 (2004).
11. J. Cho, H. Kim, H. Kim, J. W. Lee, S. Yoon, C. Sone, Y. Park, and E. Yoon, *Phys. Status Solidi C*, **2**, 2874 (2005).
12. J.-H. Lee, J. T. Oh, Y. C. Kim, and J.-H. Lee, *IEEE Photon. Technol. Lett.*, **20**, 1563 (2008).
13. H. Kudo, Y. Ohuchi, T. Jyouichi, T. Tsunekawa, H. Okagawa, K. Tadatomo, Y. Sudo, M. Kato, and T. Taguchi, *Phys. Status Solidi A*, **200**, 95 (2003).
14. C.-C. Pan, C.-H. Hsieh, C.-W. Lin, and J.-I. Chyi, *J. Appl. Phys.*, **102**, 084503 (2007).
15. K. Hiramatsu, K. Nishiyama, A. Motogaito, H. Miyake, Y. Iyechika, and T. Maeda, *Phys. Status Solidi A*, **176**, 535 (1999).
16. P. Vennéguès, B. Beaumont, V. Bousquet, M. Vaille, and P. Gibart, *J. Appl. Phys.*, **87**, 4175 (2000).
17. B. Heying, X. H. Wu, S. Keller, Y. Li, D. Kapolnek, B. P. Keller, S. P. DenBaars, and J. S. Speck, *Appl. Phys. Lett.*, **68**, 643 (1996).
18. S. J. Rosner, E. C. Carr, M. J. Ludowise, G. Girolami, and H. I. Erikson, *Appl. Phys. Lett.*, **70**, 420 (1997).
19. C. Trager-Cowan, S. McArthur, P. G. Middleton, K. P. O'Donnell, D. Zubia, and S. D. Hersee, *Mater. Sci. Eng., B*, **59**, 235 (1999).
20. O. Parillaud, V. Wagner, H.-J. Bühlmann, F. Lelarge, and M. Ilegems, *MRS Internet J. Nitride Semicond. Res.*, **5**, W3.13 (2000).
21. D. G. Zhao, S. J. Xu, M. H. Xie, S. Y. Tong, and H. Yang, *Appl. Phys. Lett.*, **83**, 677 (2003).
22. S. Hearne, E. Chason, J. Han, J. A. Floro, J. Figiel, J. Hunter, H. Amano, and I. S. T. Tsong, *Appl. Phys. Lett.*, **74**, 356 (1999).
23. A. F. Wright, *J. Appl. Phys.*, **82**, 2833 (1997).
24. W. D. Nix and B. M. Clemens, *J. Mater. Res.*, **14**, 3467 (1999).